The Meteoritical Society

Meteoritics & Planetary Science 42, Nr 7/8, 1337–1350 (2007)
Abstract available online at http://meteoritics.org

Constraints on the cooling history of the H-chondrite parent body from phosphate and chondrule Pb-isotopic dates from Estacado

Alexandra BLINOVA[1†*], Yuri AMELIN[2], and Claire SAMSON[1]

[1]Department of Earth Sciences, Carleton University, Ottawa, Ontario, Canada K1S 5B6
[2]Geological Survey of Canada, 601 Booth Street, Ottawa, Ontario, Canada K1A 0E8
[†]Present address: Department of Earth and Atmospheric Sciences, University of Alberta, Edmonton, Alberta, Canada T6G 2E3
[*]Corresponding author. E-mail: blinova@ualberta.ca

(Received 12 October 2006; revision accepted 30 March 2006)

All appendices for this article are available online at http://meteoritics.org.

Abstract–To constrain the metamorphic history of the H-chondrite parent body, we dated phosphates and chondrules from four H6 chondritic meteorites using U-Pb systematics. Reconnaissance analyses revealed that only Estacado had a sufficiently high $^{206}Pb/^{204}Pb$ ratio suitable for our purposes. The Pb-Pb isochron date for Estacado phosphates is measured to be 4492 ± 15 Ma. The internal residue-second leachate isochron for Estacado chondrules yielded the chondrule date of 4546 ± 18 Ma. An alternative age estimate for Estacado chondrules of 4527.6 ± 6.3 Ma is obtained from an isochron including two chondrules, two magnetically separated fractions, and four bulk chondrite analyses. This isochron date might represent the age of termination of Pb diffusion from the chondrules to the matrix. From these dates and previously established closure temperatures for Pb diffusion in phosphates and chondrules, we estimate an average cooling rate for Estacado between 5.5 ± 3.2 Myr/°C and 8.3 ± 5.0 Myr/°C. Using previously published results for Ste. Marguerite (H4) and Richardton (H5), our data reveal that the cooling rates of H chondrites decrease markedly with increasing metamorphic grade, in agreement with the predictions of the "onion-shell" asteroid model. Several issues, however, need to be addressed before confirming this model for the H-chondrite parent body: the discrepancies between peak metamorphic temperatures established by various mineral thermometers need to be resolved, diffusion and other mechanisms of element migration in polycrystalline solids must be better understood, and dating techniques should be further improved.

INTRODUCTION

Parent bodies of ordinary chondrites never reached their melting point, but locally experienced extensive thermal metamorphism (Dodd 1981; McSween and Sears 1988). Minerals that formed or were modified by thermal metamorphism preserve a record of the metamorphic conditions. Furthermore, if we can date these minerals, then we can reconstruct the thermal history of the parent body using the same approach as that adopted in standard methods of thermochronology (Reiners et al. 2005 and references therein).

At present there are two thermal models for the H-chondrite parent body. The first model considers assembly of still hot planetesimals of ≤10 km in radius that were heated prior to accretion into one chondrite parent body (Scott and Rajan 1981). The cooling rates are controlled by the burial depth after the accretion. A few important assumptions are required for this model to work. Prior to accretion, planetesimals had to have either a greater proportion of radionuclides or a much poorer thermal diffusivity than larger bodies in order to be sufficiently heated. Afterward, planetesimals had to accrete almost intact in order to retain sufficient heat (Grimm 1985).

The second ("onion-shell") thermal model assumes that a rocky asteroid ("parent body") about 200 km in diameter accreted cold (a rapid accretion with a duration of about 10^5 years), followed by heating due to ^{26}Al decay (Herndon and Herndon 1977; Minster and Allegre 1979; Miyamoto et al. 1981; Trieloff et al. 2003). This model predicts that petrological type 6 was in the center of the parent body and was metamorphosed in temperature range of 750–950 K. Surrounding the center of the parent body were zones composed of petrological types 5 and 4 representing

metamorphic temperatures between 700–750 K and 600–700 K, respectively (McSween 1999). The slow conduction of heat through the parent body allowed type 3 to be the least metamorphosed type on the surface. This model assumes that solid bodies existed before significant internal heating began (0.1–1.0 Myr) (Grimm 1985).

Several studies attempted to constrain the thermal history of the H-chondrite parent body by different methods: ^{244}Pu fission track (Pellas and Stozer 1975), ^{40}Ar-^{39}Ar dating (Turner et al. 1978), and integration of ^{244}Pu fission track and ^{40}Ar-^{39}Ar thermochronology on a number of unshocked H chondrites of different petrologic types (Trieloff et al. 2003). The results from the later study provided compelling evidence for the "onion-shell" model by adopting the analytical and thermal parameters of Miyamoto et al. (1981).

The rate of cooling of a metamorphic rock after passing the peak of metamorphism can be determined by dating two or more minerals if the diffusion of the radioactive element and/or its decay product in one mineral ceases at a higher temperature than in the other. Two minerals are most suitable for constraining the thermal evolution of asteroids in the high-temperature range by U-Pb dating of bulk chondrites. The first is pyroxene, the primary host of uranium in chondrules (Amelin et al. 2003), and the second is Ca phosphate (apatite and merrillite), a minor metamorphic mineral in the chondrite matrix and an important secondary host of uranium (Göpel et al. 1994). The closure temperatures of the U-Pb isotopic systems in these minerals can be estimated on the basis of experimentally determined diffusion coefficients for Pb (Cherniak et al. 1991; Cherniak 2001).

The cooling rate of the H-chondrite parent body has been recently estimated using the approach of U-Pb dating of chondrules and phosphates from the H5 chondrite Richardton (Amelin et al. 2005). A similar study using U-Pb dating of phosphates only from fifteen equilibrated ordinary chondrites was performed by Göpel et al. (1994).

A detailed thermal model of an asteroid requires, however, that the cooling rates and their links to the absolute time scale are determined for zones with various degrees of metamorphism. In this study, we examine the thermal history of H6 chondrites that experienced more intensive metamorphism than the previously dated Richardton. We present a detailed U-Pb isotopic study of the H6 chondrite Estacado and preliminary isotopic data for three other H6 chondrites. The results reported here are parts of the B.Sc. thesis of the first author (Blinova 2006) and were reported in an abstract from Blinova et al. (2006).

The main challenge in this study was the high degree of metamorphic recrystallization that made separation of chondrules barely possible. Therefore, we attempted to obtain chronological information from analyses of bulk silicate in addition to the limited amount of chondrule data. The interpretation of the bulk chondrite data is model dependent, and U-Pb dating of bulk chondrite requires further experiments and modeling before it can be considered a reliable dating method. However, a combination of chondrule and bulk silicate U-Pb data can potentially allow to see through the post-metamorphic cooling and to determine the timing of the peak of metamorphism, or possibly the timing of chondrule formation for equilibrated chondrites.

EXPERIMENTAL PROCEDURES

Meteorite Selection

For this study, we selected four H6 chondrites from the National Meteorite Collection of Canada (NMCC) hosted at the Geological Survey of Canada in Ottawa. Among the chondrites available in sufficient quantities, we chose Dresden, Estacado, Great Bend, and Mount Browne as the least shocked (shock stage 1–3 based on the Stöffler-Keil-Scott shock stage classification [Stöffler et al. 1991; data summarized by Grady 2000]) and least weathered (degree of weathering 0–3 [Grady 2000]) meteorites [Table A1, available online at http://meteoritics.org]. The rationale for choosing these meteorites was to study samples primarily affected by metamorphism and not by subsequent events.

Sample Preparation

Using a scanning electron microscope, we visually identified olivine and pyroxene, which are the main constituents of chondrules, and chloroapatite and merrillite, i.e., phosphate minerals (elemental map, Appendix 1, available online at http://meteoritics.org).

Subsequently, we crushed each sample with a hydraulic press and then sieved them. Three fractions were obtained for all four meteorites upon sieving: coarse-grained (>300 μm), medium-grained (300–153 μm), and fine-grained (<153 μm) fractions. Chondrules were picked out from the coarse-grained fraction of each sample. However, the yield of intact chondrules or clearly recognizable fragments after crushing was much smaller than for chondrites of a lower metamorphic grade as a result of extensive recrystallization of H6 chondrites. For example, from Estacado (Fig. 1) we could get only one intact chondrule and four clearly identifiable chondrule fragments (one fraction) suitable for U-Pb analyses. The samples were crushed further to the medium-grained size. The phosphate fractions were separated by magnetic susceptibility from both the medium-grained and fine-grained fractions using a Frantz Magnetic Barrier Separator LB-1 (Fig. 2).

Sample Washing, Chemical Separations, and Mass Spectrometry

Because of the difference in physical and chemical properties between the phosphate and silicate minerals in

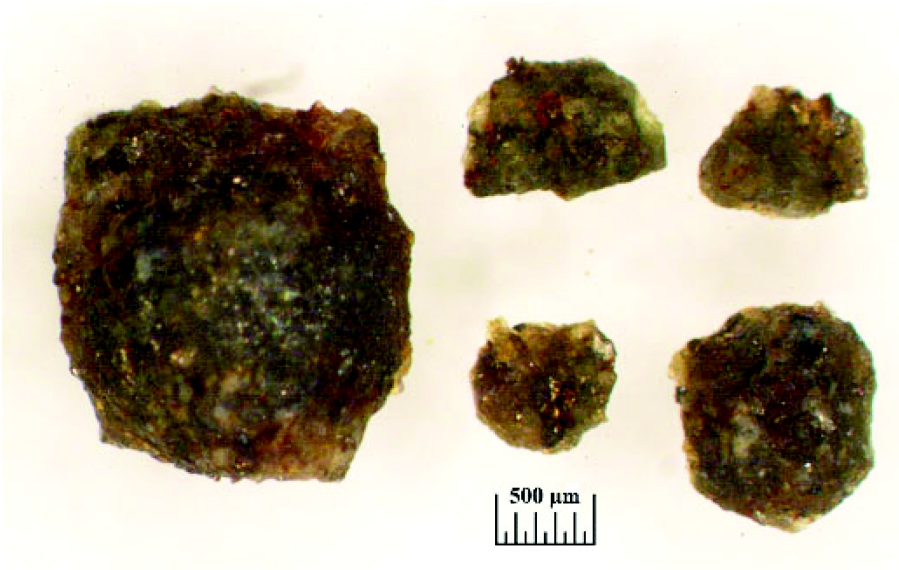

Fig. 1. Estacado chondrules.

chondrites, we used different versions of the washing and chemical separation procedures for these materials. The mass spectrometry procedures were identical. All fractions were spiked with the mixed ^{202}Pb-^{205}Pb-^{233}U-^{235}U spike (Amelin and Davis 2006) before dissolution.

We washed the separated phosphates in distilled acetone but did not perform acid leaching. To each sample, we added 220 mg of 3M HCl and left it overnight to dissolve. Uranium and Pb fractions were separated using columns containing 0.05 ml of the Bio-Rad AG1X8 resin. Both elements were collected from a single column pass in 0.2M HBr–0.5M HNO_3 and 0.03M HBr–0.5M HNO_3, respectively (procedure modified from Lugmair and Galer 1992), and evaporated with H_3PO_4 before loading on the mass spectrometer filaments.

Chondrite silicates (chondrules, pyroxene- and olivine-rich magnetically separated fractions, and crushed bulk meteorite) required more complex washing and chemical separations. Silicate fractions were analyzed in several analytical sessions during the course of this study, and we tried various versions of the washing procedure in a search for the most efficient way of removing common Pb (here all Pb other than in situ accumulated radiogenic Pb, or radiogenic Pb being transferred from its growth site, is referred to as common Pb). The details of the washing procedure are described in Appendix 2 (available online at http://meteoritics.org). The chemical separation procedure was modified as well. The original procedure was developed for processing chondrules less than 5 mg in weight (Amelin et al. 2005). In the analyses of magnetically separated and bulk meteorite fractions, we used larger amounts of material (up to ~40 mg) to achieve stronger ion beams and hence higher precision. However, the yield for Pb and U, and the efficiency of separation were compromised if the original procedure

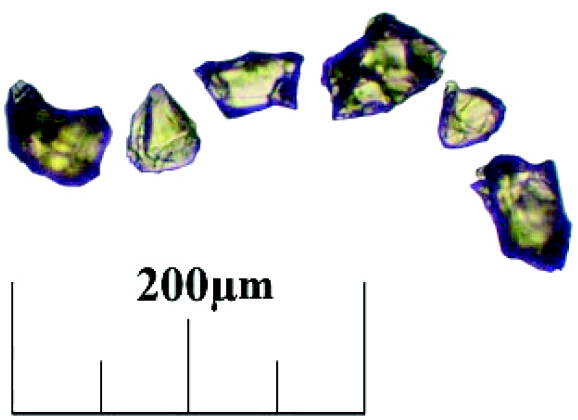

Fig. 2. Estacado phosphates.

were used for larger fractions. At a later stage of work, we used a modified procedure optimized for larger fractions. To reduce the matrix to sample ratio, both Pb and U, separated using a procedure similar to the phosphate chemistry described above, were additionally purified by repeated passing through the same columns. Details are presented in Appendix 2.

Isotopic analyses were performed at the Geological Survey of Canada in Ottawa using the TRITON multicollector thermal ionization mass spectrometer. We analyzed fractions of the NIST standard SRM-981, spiked with the same mixed tracer as the samples, with each set of Pb loads. The mass spectrometry has recently been described in detail by Amelin and Davis (2006).

We measured each Pb fraction first in a static mode using Faraday cups to obtain $^{204}Pb/^{206}Pb$ and $^{207}Pb/^{206}Pb$ values, and then ran them in dynamic mode using an electron multiplier to obtain $^{205}Pb/^{204}Pb$ ratios. During the static

analysis, the $^{204}Pb/^{206}Pb$ and $^{207}Pb/^{206}Pb$ ratios were normalized on-line relative to the measured $^{202}Pb/^{205}Pb$ ratio. Both phosphate and silicate uranium samples were run in dynamic mode measuring ^{235}U and ^{238}U.

We measured blanks for each step of the procedure (washing, digestion, chemical separation) using a ^{230}Th-^{235}U-^{205}Pb spike along with each batch of samples. The blank values are summarized in Appendix 2. Total blanks for each session were calculated as the sum of the blanks for individual steps, therefore the total blanks for washes (the sum of the wash blank and the separation blank) and for residues (the sum of the digestion blank and the separation blank) in the same batch are usually different. An 80% uncertainty in the blank values, determined from long-term reproducibility of blanks, was propagated into the errors of Pb-isotopic and U-Pb errors. Including blank uncertainty in the error propagation has major effect on the errors of Pb-isotopic ratios for the fractions in which analytical blank comprises large portion of the total common Pb: it greatly increases the errors of $^{204}Pb/^{206}Pb$ and $^{207}Pb/^{206}Pb$ ratios, and makes their errors strongly correlated. The influence of this source of error on the uncertainty of isochron dates and model dates is, however, small if the error correlations are recalculated accurately. The effect of the blank uncertainty on larger fractions, and on the fractions containing more common Pb, is small.

Isotopic ratios corrected for fractionation on-line and uncorrected were collected and further reduced off-line. Final isotopic ratios corrected for fractionation, blank, and spike, and their errors and error correlations, were calculated using the PBDAT program (Ludwig 1993). Isochrons, weighted means and medians, and their uncertainties were calculated using Isoplot/Ex version 3.00 (Ludwig 2003). All isochrons and weighted mean and median errors have 95% confidence intervals, unless indicated otherwise.

RESULTS

Reconnaissance U-Pb Data for H6 Chondrites

Based on suggestions by Faure (1986) and referenced in Amelin (2006), the term “age” is applied here to any period between a geological event and the present, while the term “date” is the calculated time utilizing the law of radioactive decay.

Complete U-Pb data for phosphate and silicate (chondrules, pyroxene- and olivine-rich magnetically separated fractions, and crushed bulk meteorite) fractions for the chondrites Dresden, Estacado, Great Bend, and Mount Browne are in Table A3 (available online at http://meteoritics.org). In order to select the most appropriate meteorite for detailed study, we started with reconnaissance dating of two phosphate fractions and two silicate fractions (and their washes) from each meteorite (phosphate fractions #6 and 7 in Estacado, #1 and 2 in other meteorites; silicate fractions #1R and 2R in all meteorites) (Table A3). We were looking for a meteorite with a sufficiently high radiogenic Pb isotopic composition (high $^{206}Pb/^{204}Pb$) in both phosphates and acid-washed silicates. These reconnaissance analyses yielded relatively high values of $^{206}Pb/^{204}Pb$ (between 150.1 and 764.5) in silicate fractions from all four meteorites, suggesting that precise and accurate dating of chondrules/silicates may be possible. Phosphate analyses yielded more diverse data. Two analyses from Estacado yielded relatively high $^{206}Pb/^{204}Pb$ of 181.7 and 67.99. The phosphate fractions from Mount Browne yielded $^{206}Pb/^{204}Pb$ of 78.31 and 23.64, whereas Pb in phosphates from Dresden ($^{206}Pb/^{204}Pb$ of 24.40 and 23.51) and Great Bend ($^{206}Pb/^{204}Pb$ of ~19 in both fractions) is substantially less radiogenic.

On the basis of these data, we chose Estacado as the best among the four tested H6 chondrites for a detailed thermochronological study. Mount Browne would be our second best choice for a similar study due to phosphates displaying more radiogenic Pb than Dresden and Great Bend. The calculated Dresden chondrule date of 4555 Ma (for 4 and/or 6 fractions) is within the range of expected values for the primary age of chondrites (Amelin et al. 2002). However, rather unradiogenic and almost invariable Pb isotopic composition in phosphates from Dresden, as well as Great Bend, precludes getting reliable Pb-Pb isochron dates from these minerals, and this essentially disqualifies these meteorites as candidates for a thermochronological study. These meteorites may be, however, suitable for a future chronological study of chondrules.

Isochron regressions for Dresden, Great Bend, and Mount Browne, shown in Table 2, exhibit a variety of phosphate and chondrule dates. Some isochrons are based on two points only (phosphate and residue isochrons), while others are based on highly scattered arrays of 3–4 points (combined residue-leachate isochrons for the silicates). Therefore, the dates calculated from such isochrons may be unreliable and should not be used as actual dates. Additional U-Pb work is necessary to confirm the calculated chondrule dates from these meteorites.

Detailed U-Pb Data for the Estacado Chondrite

Phosphate fractions in Estacado contain from 0.714 to 2.79 parts per million (ppm) of uranium (Table 1). The highest uranium concentration is found in fraction #6. This value is similar to the values reported by Göpel et al. (1994). Uranium concentrations in acid-washed chondrite silicate fractions vary from 1 to 40 parts per billion (ppb). These results are comparable to values reported by Amelin et al. (2005) for the Richardton meteorite.

Phosphate fractions contain moderate concentrations of total Pb (Table 1). These values vary from 2.40 to 9.65 ppm. Acid-washed bulk silicate fractions contain smaller

Table 1. Estacado Pb data.

Fraction number	Fraction description[a]	ppm U	ppm Pb	$^{204}Pb/^{206}Pb$ (total)	$^{204}Pb/^{206}Pb$ % err	$^{207}Pb/^{206}Pb$ (total)	$^{207}Pb/^{206}Pb$ % err	Rho 4/6–7/6	$^{207}Pb^*/^{206}Pb^*$ date (Ma)	$^{207}Pb^*/^{206}Pb^*$ date err	$^{207}Pb^*/^{235}U$	$^{207}Pb^*/^{235}U$ % err	$^{206}Pb^*/^{238}U$	$^{206}Pb^*/^{238}U$ % err	Rho 6/8–7/5	Percent discordance[b]
Phosphates																
1	ES mg1	0.861	6.15	0.03229	0.225	0.7447	0.011	0.147	4482.2	1.2	145.762	0.474	1.7935	0.450	0.985	–79
2	ES mg2	1.24	9.65	0.03291	0.329	0.7488	0.006	0.0720	4486.1	1.8	151.199	0.507	1.8555	0.452	0.972	–85
3	ES nm1	1.35	4.35	0.01707	0.179	0.6809	0.018	0.835	4509.5	0.23	102.170	0.611	1.2337	0.611	1.000	–22
4	ES nm2	1.02	2.83	0.01325	0.347	0.6612	0.033	0.800	4504.7	0.38	97.200	0.605	1.1776	0.605	0.999	–16
5	ES nm3	1.17	3.01	0.01138	0.370	0.6504	0.028	0.975	4499.4	0.12	94.193	0.311	1.1453	0.312	1.000	–13
6	ON3	2.79	5.73	0.00548	0.349	0.6227	0.017	0.477	4500.1	0.26	88.158	0.215	1.0715	0.214	0.996	–6
7	ON4	0.714	2.40	0.01466	0.552	0.6638	0.063	0.0960	4493.2	1.5	98.733	0.612	1.2057	0.594	0.985	–20
Silicates																
2-R	TP2	0.0041	0.0165	0.00597	7.78	0.6441	0.289	0.966	4548.4	1.4	106.50	1.35	1.2520	1.36	0.997	–22
3-R	ES-1	0.0011	0.0061	0.00941	68.5	0.6654	3.630	0.997	4562.7	13	134.1	17.5	1.561	18.0	0.999	–52
5-R	ES-3	0.0034	0.0143	0.00440	34.3	0.6442	0.889	0.996	4566.1	2.9	114.97	5.40	1.3352	5.45	0.999	–30
6-R	ES-4	0.0007	0.0034	0.00221	212	0.6395	2.740	0.997	4578.1	8.5	132.3	13.4	1.524	13.6	0.999	–47
7-R	ES-5	0.0022	0.0103	0.00649	19.5	0.6554	0.719	0.996	4570.5	2.5	120.62	3.92	1.3965	3.98	0.999	–35
9-R	ES-7	0.0016	0.0071	0.00595	17.7	0.6572	0.584	0.997	4580.8	2.1	118.46	3.92	1.3619	3.96	0.999	–32
10-R	ES-8	0.0022	0.0110	0.00605	18.9	0.6510	0.664	0.998	4564.5	2.1	134.60	3.04	1.5649	3.09	0.999	–52
11-R	ES Ch1	0.0033	0.0115	0.00226	95.3	0.6257	1.380	0.998	4544.8	3.3	99.392	4.75	1.1714	4.85	0.999	–14
12–R	ES Ch2	0.0017	0.0062	0.00394	104	0.6359	2.540	0.996	4551.0	7.1	96.129	9.81	1.128	10.0	0.999	–10
13-R	ES 3	0.0021	0.0113	0.02214	6.77	0.7724	0.372	0.975	4701.2	8.3	122.81	5.51	1.2988	5.80	0.996	–21
14-R	ES 4	0.0033	0.0151	0.01065	13.9	0.6917	0.694	0.995	4615.4	4.0	116.81	3.91	1.3111	4.03	0.998	–25
1-W1	TP1 wash 1	0.0175	0.1345	0.04620	0.268	0.7911	0.021	0.000600	4390.7	3.0	105.537	0.415	1.38264	0.217	0.976	–42
2-W1	TP2 wash 1	0.0176	0.1342	0.04707	0.0445	0.7896	0.017	0.159	4362.2	0.77	101.52	3.45	1.35617	3.45	1.000	–40
1-W2	TP1 wash 2	0.0001	0.0014	0.04333	0.471	0.7957	0.094	0.0520	4473.7	1.8	183.58	3.68	2.27194	3.71	0.999	–127
2-W2	TP2 wash 2	0.0002	0.0038	0.03901	1.77	0.7886	0.267	0.886	4526.4	5.6	271.83	8.13	3.2445	8.26	0.999	–219
11-W1	ES Ch1 wash 1	0.0029	0.0940	0.05337	0.0235	0.8589	0.018	0.940	4543.8	0.77	398.90	1.03	4.70449	1.05	0.999	–360
12-W1	ES Ch2 wash 1	0.0065	0.0765	0.04251	0.321	0.7950	0.057	0.823	4487.1	1.3	185.39	1.60	2.2734	1.62	0.999	–126
13-W1	ES 3 wash 1	0.0298	0.2222	0.03470	0.100	0.7598	0.018	0.910	4495.1	0.22	143.686	0.231	1.752	0.235	0.998	–74
14-W1	ES 4 wash 1	0.0176	0.2067	0.04237	0.0582	0.8015	0.010	0.924	4515.7	0.27	191.717	0.291	2.305	0.298	0.998	–127
11-W2	ES Ch1 wash 2	0.0014	0.0042	0.03795	5.95	0.7997	0.615	0.930	4584.3	20.1	50.3	18.3	0.57709	19.1	0.998	44
12-W2	ES Ch2 wash 2	0.0007	0.0255	0.05252	0.256	0.8557	0.158	–0.191	4547.0	7.3	469.93	9.34	5.53	9.56	0.999	–440
13-W2	ES 3 wash 2	0.0004	0.0029	0.03486	11.4	0.7970	0.971	0.938	4620.7	32.9	150.2	27.3	1.680	28.8	0.998	–60
14-W2	ES 4 wash 2	0.0002	0.0040	0.04093	4.83	0.8048	0.564	0.898	4554.2	20.0	260.4	21.8	3.050	22.6	0.999	–197
CDT	Primordial Pb			0.1074	0.0002	1.1060	0.0006	0.0000								
SK_0	Modern S-K Pb			0.0535	0.0001	0.8356	0.0004	0.0000								
	Blank			0.0538	0.5920	0.8315	0.2000	0.0000								

[a]For complete fraction description, see Table A3.

[b]Calculated using the formula: $100 \times [(\exp((\lambda 238) \times Age^{207}Pb^*/^{206}Pb^*) - 1) - {}^{206}Pb^*/^{238}U]/[\exp((\lambda 238) \times Age^{207}Pb^*/^{206}Pb^*) - 1]$.

*Corrected for fractionation, spike, blank, and primordial Pb isotopic composition from Tatsumoto et al. (1973).

nd = not determined.

Isotopic ratios are corrected for fractionation, blank, and spike.

Errors are 2 sigma of the mean.

Dates calculated using the primordial Pb isotopic composition from Tatsumoto et al. (1973).

Table 2. Summary of Pb-Pb isochron calculations.

Sample	Fractions	Residues and/or washes	Fractions included in regression (keyed to Table 1 for Estacado and online Table A3 for other meteorites)	Total number of fractions used in calculations (n)	$^{204}Pb/^{206}Pb$-$^{207}Pb/^{206}Pb$ date (Ma)	2σ date err.	MSWD	Weighted average $^{207}Pb/^{206}Pb$	2σ date err.	MSWD
Estacado	Phosphates									
	All fractions		1–7	7	4497.0	13	1346	4501.5	4.3	0.64
	Only nonmagnatic		3–7	5	4492.0	15	737	4501.7	4.3	0.81
	Silicates									
	Chondrules	Residue + wash 2	11R, 12R, 11W2, 12W2	4	4546.0	18	7			
	Bulk chondrite I	Residue + wash	19R–22R, 19W–22W	8	4572.0	12	222			
	Bulk chondrite II	Residue + wash + untreated sample	15, 17, 18, 19R-22R, 19W–22W	11	4570.0	19	621			
	Chondrules + magnetic fractions	Residues	11R–14R	4	4532.0	16				
	Chondrules + magnetic fractions + bulk chondrite	Residues	11R–14R, 19R–22R	8	4527.6	6.3	1.11			
	Bulk silicate (magnetic fractions)	Residues (excluding two fractions)	1R, 3R–8R, 10R	8	4533.0	64	2.8	4563.0	13	0.042
	Bulk silicate (magnetic fractions)	Residues + wash 1, 2	1R–10R + 1W1–W2, 2W1–2	14	4577.0	10	1554	4531.0	42	9.9
	Bulk silicate (magnetic fractions)	Residues + wash 2	1R–10R + 1W2, 2W2	12	4569.1	4.6	242	4560.0	13	0.46
	Bulk silicate (magnetic fractions)	Residues (excluding two fractions) + wash 2	1R, 3R–8R, 10R + 1W2, 2W2	10	4569.6	2.9	88	4560.0	14	0.52
Great Bend	Phosphates									
	All fractions		1–2	2	nd	nd	nd	4480.0	1100	0.0014
	Silicates									
	Bulk silicate (magnetic fractions)	Residues	1R–2R	2	4487.5	0.78	na	4491.0	13	0.043
	Bulk silicate (magnetic fractions)	Residues + wash 1, 2	1R–2R + 1W1–W2, 2W1–W2	6	4492.0	14	1031	4488.0	13	0.74
	Bulk silicate (magnetic fractions)	Residues + wash 2	1R–2R + 1W2, 2W2	4	4490.3	6.7	94	4491.0	13	0.038
Dresden	Phosphates									
	All fractions		1–2	2	4848.0	65	nd	4562.0	140	0.016
	Silicates									
	Bulk silicate (magnetic fractions)	Residues	1R–2R	2	4558.0	6.7	na	4555.3	8	0.00037
	Bulk silicate (magnetic fractions)	Residues + wash 1, 2	1R–2R + 1W1–W2, 2W1–W2	6	4554.6	0.60	5.1	4555.4	8	0.072
	Bulk silicate (magnetic fractions)	Residues + wash 2	1R–2R + 1W2, 2W2	4	4554.8	0.86	3.6	4555.4	8	0.027
Mount Browne	Phosphates									
	All fractions		1–2	2	4568.6	1.6	na	4543.0	53	0.79
	Silicates									
	Bulk silicate (magnetic fractions)	Residues	1R–2R	2	4559.3	1.6	na	4554.0	14	0.019
	Bulk silicate (magnetic fractions)	Residues + wash 1, 2	1R–2R + 1W1, 2W1–W2	5	4551.0	18	935	4558.0	35	3.4
	Bulk silicate (magnetic fractions)	Residues + wash 2	1R–2R + 1W2, 2W2	4	4551.0	5.3	44	4558.0	46	4.6

na = not applicable.
nd = not determined.

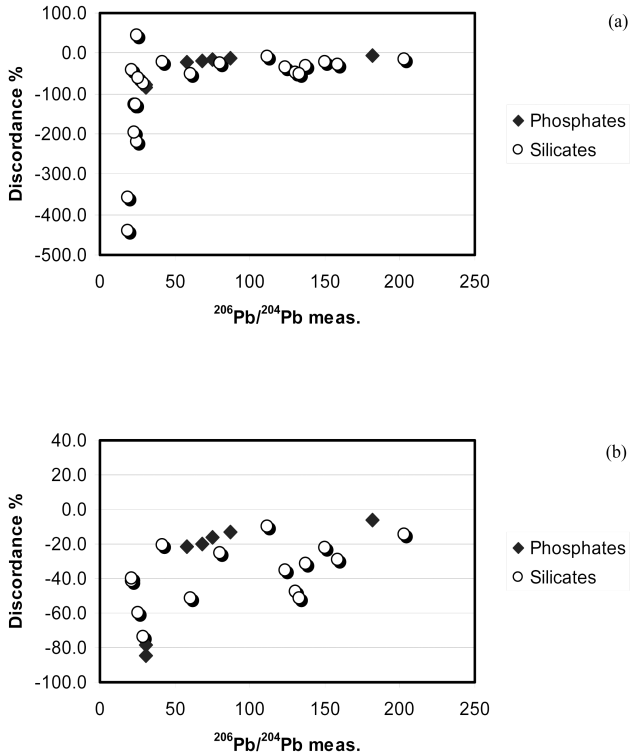

Fig. 3. a) $^{206}Pb/^{204}Pb$ measured versus percent of discordance for Estacado phosphates and silicate fraction (only samples with measured U). b) Close-up of fractions with discordance less than 100%.

concentrations of Pb between 3.44 to 16.5 ppb. The measured $^{206}Pb/^{204}Pb$ ratio ranges from 30.36 to 181.7 for phosphates and from 41.69 to 212.4 for bulk silicates (Table A3). Phosphate values are comparable to those of the Richardton meteorite, but bulk silicate values are lower than in Richardton (Amelin et al. 2005).

Uranium-lead model dates in Estacado phosphates (Table 1) are variably discordant. The degree of discordance decreases with increasing $^{206}Pb/^{204}Pb$ ratio (Figs. 3a and 3b). The fraction containing the most radiogenic Pb is only 6% discordant. This suggests that U-Pb systems in Estacado phosphates were probably closed, and that inaccurate subtraction of "initial" Pb is the main source of discordance.

The measured $^{206}Pb/^{204}Pb$ ratios in bulk silicate washes are much lower than residues (Table A3). Amounts of common Pb are high in first washes (226–3397 pg) and become progressively lower in second washes (11.9–83.5 pg) (Table A3).

The results of Pb-Pb isochron and model dates for all meteorites used in this study are summarized in Table 2. A composite $^{204}Pb/^{206}Pb$ versus $^{207}Pb/^{206}Pb$ diagram for Estacado silicates and phosphates is presented in Fig. 4. The Pb-Pb isochron date for all phosphate fractions (n = 7) is 4497 ± 13 Ma. An isochron for five non-magnetic fractions (after excluding magnetic fractions #1–2 that contain twice the

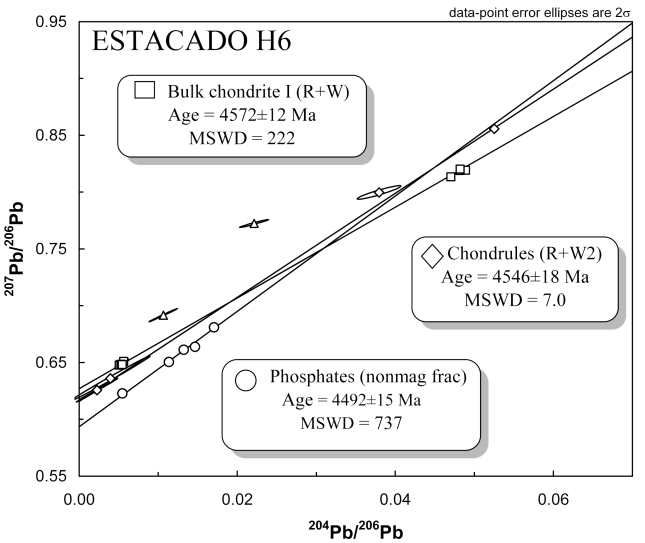

Fig. 4. Composite $^{204}Pb/^{206}Pb$ versus $^{207}Pb/^{206}Pb$ diagram for Estacado silicates and phosphates. Circles = phosphate non-magnetic fractions only. Diamonds = chondrules (residues and wash 2). Squares = bulk chondrite fractions I (Table 2) (residues and washes). Triangles = magnetically separated silicate fractions.

amount of common Pb compared to non-magnetic fractions, possibly as a result of leaching from residual feldspar) yields the date of 4492 ± 15 Ma, which we consider the best age estimate for the Estacado phosphates (Fig. 4).

We were able to separate and analyze only two chondrule fractions (#11R, one large chondrule, and #12R, four unambiguous chondrule fragments) (Table 1; Fig. 1). Due to the high metamorphic grade of Estacado, the chondrules were mostly destroyed by metamorphism, with a few exceptions of locally preserved intact chondrules (Fig. 1). The internal residue-second leachate isochron for chondrules gives Pb-Pb date of 4546 ± 18 Ma (MSDW = 7), which we consider the best age estimate for the Estacado chondrules (Fig. 4). A bulk chondrite (residues and washes) Pb-Pb isochron regression gives a consistently higher date of 4572 ± 12 Ma (MSDW = 222) (Fig. 4). Including untreated fractions #15R–18R does not change the age but increases data scattering. Analyses of bulk silicates during the reconnaissance study (#1R-10R and second wash) (Table 2) yielded Pb-Pb date of 4569.1 ± 4.6 Ma (MSDW = 242). These fractions, similar to fractions #13R–14R, were magnetically separated material. They are neither chondrules nor strictly the bulk chondrite, but a mixture of chondrule and matrix material. Such a mixture would not necessarily have the same proportions of components as the bulk chondrite. This is probably due to the variable abundances of finely dispersed highly magnetic minerals in both chondrules and matrix which get partially fractionated during magnetic separation. Therefore, the dates yielded by different combinations of these fractions (4533 ± 64 to 4569.6 ± 2.9) (Table 2) would be questionable.

The U-Pb system in chondrules is nearly concordant, whereas other silicate fractions show variable degrees of discordance (Figs. 3a and 3b) despite a relatively high $^{206}Pb/^{204}Pb$ ratio. Most silicate fractions with $^{206}Pb/^{204}Pb$ ratios between 50–250 are more discordant than phosphate fractions with similar $^{206}Pb/^{204}Pb$ ratios (Table 1). This additional discordance is probably related to fractionation between radiogenic Pb and U during acid leaching.

The reasons for the noticeable age difference between the chondrules and the bulk chondrites are not obvious. In order to understand this discrepancy, we need to discuss the behavior of the U-Pb system during chondrite metamorphism.

DISCUSSION

Common Pb in Estacado Phosphates and Chondrules

Pb in phosphate and silicate fractions from Estacado chondrite analyzed here is a mixture of radiogenic Pb produced in situ, and one or more additional components, such as initial Pb, terrestrial contamination, or Pb redistributed in the parent asteroid by metamorphism, alteration, and/or impacts. We collectively refer to these additional components as common Pb. Isotopic composition of common Pb cannot be directly determined from analyses of fractions that contain mixed Pb, or from Pb-Pb isochron regressions of such fractions. It is possible, however, to infer the possible presence of these common Pb components from the relative position of a Pb-Pb isochron and known Pb isotopic composition of likely components, such as primordial Pb and modern terrestrial Pb (approximated here by Pb in Canyon Diablo troilite [CDT] [Tatsumoto et al. 1973] and zero-age Pb in Stacey and Kramers [1975] model [SK_0], respectively).

Pb-Pb isochrons (with 2σ error envelopes) for Estacado silicates and phosphates are plotted together with primordial Pb and modern terrestrial Pb in Appendix 4. The error envelopes of phosphate isochrons, including either non-magnetic fractions (Fig. A1a) or all fractions (Fig. A1b) in Appendix 4 pass close to the point of primordial Pb, and the isochron including magnetic fractions also overlaps modern terrestrial Pb. The bulk chondrite I (residue + wash) isochron (Fig. A1c in Appendix 4) passes through modern terrestrial Pb, and stays distinctly below the primordial Pb. The chondrule residue and second wash isochron goes through the point of primordial Pb, and stays above the modern terrestrial Pb (Fig. A1d in Appendix 4). First washes of the same chondrules plot closer to the modern terrestrial Pb.

This pattern suggests that common Pb in Estacado consists of at least two components. The first is modern common Pb of either terrestrial or possibly extraterrestrial (e.g., Pb volatilized during a recent collision that excavated the meteoroid material from its parent asteroid) origin. The second is either primordial Pb, or a component with $^{207}Pb/^{206}Pb$ even higher than in primordial Pb, produced by radiogenic growth in a system with high μ ($^{238}U/^{204}Pb$) since the formation of the asteroid and until the event that removed this radiogenic Pb (which is referred hereafter as "aborted high-μ Pb") from its host minerals and distributed it elsewhere. An isochron that passes above the point of primordial Pb suggests the presence of aborted high-μ Pb. None of the four isochrons discussed earlier in this section passes above primordial Pb outside of the error, therefore these data do not provide clear evidence for the presence of aborted high-μ Pb. Such evidence is provided by analyses of magnetically separated silicate fractions discussed below.

Age of the Estacado Chondrules—The Timing of Termination of Pb Diffusion in Pyroxene

The presence of multiple common Pb components and secondary alteration effects can complicate the determination of a precise and accurate Pb isotopic age. Such difficulty can be potentially overcome by including Pb isotopic composition of acid leachates (washes) in age calculations (Krot et al. 2005; Amelin and Krot, Forthcoming).

Residue-leachate isochrons can be effectively used for age determination. If a chondrule contains two or more common Pb components of variable solubility, then it can be expected that some of these components are more easily leached by acids than others. Sequential acid leaching would produce a series of fractions containing common Pb with variable isotopic composition, which may also differ from the common Pb isotopic composition in the residue. The two point isochron for "residue + second leachate" pairs can be expected to yield more accurate dates, because the more soluble common Pb component is removed by the first leaching step, whereas the second leachate and residue contain relatively insoluble Pb components (Krot et al. 2005).

The internal residue-second leachate isochron date of 4546 ± 18 Ma (MSDW = 7) gives us a relatively precise estimate of the age of chondrules. Since the closure temperature for Pb diffusion in chondrule pyroxenes (estimated at 782 ± 106 °C by Amelin et al. [2005] on the basis of the experimental diffusion data of Cherniak [2001]), is lower than the estimated peak temperature reached by H6 chondrites (865–926 °C, estimated by Slater-Reynolds and McSween [2005] from two-pyroxene thermometry), the date of 4546 ± 18 Ma is interpreted as the timing of termination of Pb diffusion in chondrule pyroxene.

The Significance of the Bulk Silicate Pb-Isotope Data, and an Alternative Estimate of the Timing of Cessation of Pb Diffusion

In the Pb-Pb isochron diagrams (Figs. 4 and 5), the data points of acid-washed bulk meteorite plot above the

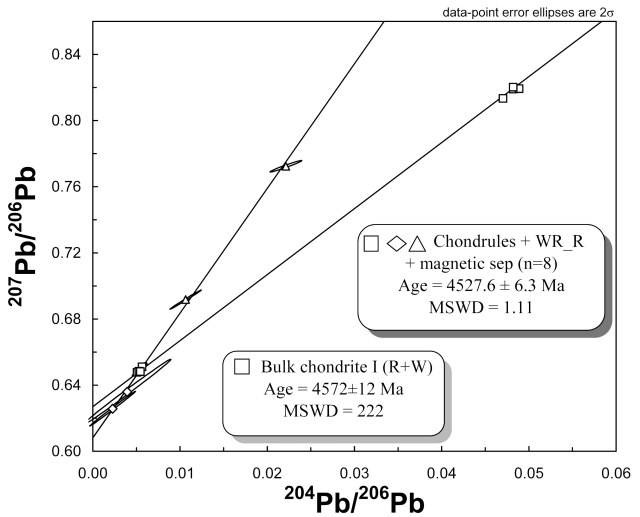

Fig. 5. $^{204}Pb/^{206}Pb$ versus $^{207}Pb/^{206}Pb$ diagram for Estacado chondrules, whole rock, and magnetically separated fractions, showing intersecting whole rock residue-wash isochron and a regression line through chondrule, whole rock, and magnetic fraction data, which is interpreted as a radiogenic Pb transfer isochron. Symbols are the same as in Fig. 1.

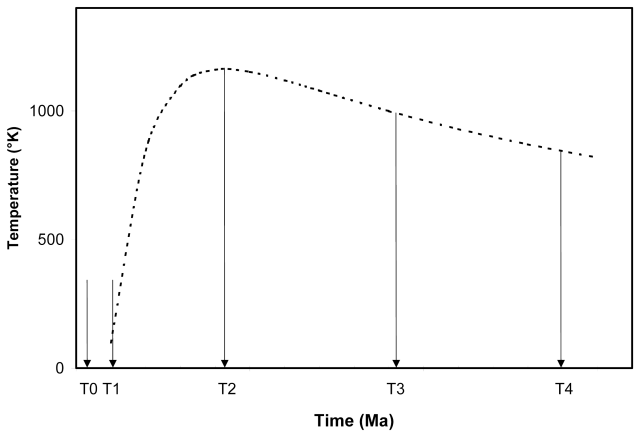

Fig. 6. Schematic presentation of the thermal history of H6 chondrites showing the main events and their manifestation in the U-Pb systematics. T0 = formation of chondrules and other chondritic components. T1 = accretion. Assumed to be instantaneous (although this assumption is not strictly true, e.g., Ghosh et al. 2003). This event is not directly recorded in the Pb isotopic systematics. T2 = peak of metamorphism; formation of phosphates; partial loss of volatiles, including common Pb, and perhaps a part of radiogenic Pb accumulated by that time. The U-Pb isotopic system in the bulk rock is considered closed at this point. T3 = closure of Pb diffusion in pyroxene; cessation of the leakage of radiogenic Pb from the chondrules to the matrix. The U-Pb isotopic system in pyroxene and in chondrules is considered closed since that moment. T4 = closure of Pb diffusion in phosphates. The U-Pb isotopic system in the chondrite and in all its components is considered closed since that moment.

chondrule residue-leachate isochron, and have model dates identical to the ages of chondrules in primitive chondrites (Amelin et al. 2002; Amelin and Krot, Forthcoming) and close to the age of the earliest dated solids in the solar system. Two magnetically separated fractions (#13-R and 14-R) (Table 1) plot even higher in the isochron diagram (triangles in Fig. 4), and have unreasonably old single-stage model dates and leachate-residue isochron dates well over 4.6 Ga. The origin of anomalously high $^{207}Pb/^{206}Pb$ in these fractions is hard to explain, unless these fractions contain minerals that captured early radiogenic Pb, accumulated elsewhere in the chondrite, i.e., aborted high-μ Pb.

In order to interpret the Pb-isotopic data for bulk chondrites, we will consider a chondrite as a simple three-reservoir system. This hypothetical chondrite consists of two reservoirs of high-temperature minerals with different geochemical properties: "chondrules" that contain a certain amount of U but did not incorporate common Pb during their formation, and "matrix" that contains a certain amount of initial Pb but no U. The "chondrules" and "matrix" as model geochemical reservoirs do not exactly match the real chondrules and matrix (petrologic entities) in chondrites, but provide a useful approximation. Besides these high-temperature reservoirs, our hypothetical chondrite contains a low-temperature reservoir enriched in Pb over U relative to the bulk chondrite concentrations, which we label "interstitial" material. The Pb in this reservoir is mainly brought by the shock-induced redistribution of volatiles during asteroid breakup, as well as by terrestrial weathering, and by handling in the museum and laboratory. We assume that the loosely bound Pb in chondrites, which is extracted during the first leaching step in dilute acid, comes from the "interstitial" reservoir.

Soon after accretion, the chondrite parent asteroid reaches the peak of metamorphism (Fig. 6). The temperature in parts of the asteroid is sufficiently high for volatile elements (including Pb) to be partially or completely lost. The modification of the U-Pb system in this process can be described by the classical multi-stage U-Pb evolution (Gale and Mussett 1973; Tera and Carlson 1999; Tera 2003) as a two-stage evolution with lower μ ($^{238}U/^{204}Pb$) in the first stage, and increasing μ toward the second stage because of the higher volatility of Pb relative to U (e.g., Lodders 2003). A single-stage $^{207}Pb/^{206}Pb$ model date of the rock (or a Pb-Pb isochron date of whole rock samples, which is also calculated assuming a single-stage evolution) in such a system is between T0 and T2, and approaches T2 (Fig. 6) with an increasing ratio of second-stage μ over first-stage μ, in other words, with an increasing degree of volatile depletion.

A Pb-Pb isochron based on multiple analyses of acid-washed bulk meteorite fractions and their leachates (19R–22R, 19W–22W) from Estacado yielded the date of 4572 ± 12 Ma (Fig. 4). Adding the analyses of unwashed bulk chondrites (fractions 15, 17, 18) increases the data scattering, but does not appreciably change the date (isochron date is 4570 ± 19 Ma). This Pb-Pb bulk chondrite age is coeval,

Table 3. Summary of residue-wash Pb-Pb isochron calculations for individual fractions.

				Three-point isochron			Residue + HNO_3 wash		Residue + HCl wash	
Fraction (keyed to Table 1)	206/204 residue	207*/206* model date (Ma)	207*/206* model date error	Date	2σ error (Ma)	MSWD	Date	2σ error (Ma)	Date	2σ error (Ma)
11-R	442.3	4544.8	3.3	4545	77	14	4544.8	3.2	4543.1	4.9
12-R	253.5	4551.0	7.1	4368	2100	278	4554.8	4.1	4551.1	7.0
13-R	45.2	4701.2	8.3	4938	1000	37	4912.0	21	4790.1	9.7
14-R	93.9	4615.4	4.0	4635	52	24	4634.8	1.7	4628.4	3.9
19-R	197.2	4567.2	1.8				4573.1	1.7		
20-R	177.1	4569.1	3.6				4576.6	3.6		
21-R	188.9	4566.5	1.0				4572.3	0.85		
22-R	183.4	4564.2	1.4				4570.7	1.4		
Chondrule weighted mean		4545.87		4544.76			4548.59		4545.73	
2 sigma% err. of mean		1.49		38.47			61.63		2.01	
MSWD		2.51		0.03			14.79		3.51	
Rejected		0		0			0		0	
Probability of fit		0.11		0.87			0.00		0.06	
Bulk rock weighted mean		4566.10					4572.22			
2 sigma% err. of mean		2.36					2.07			
MSWD		4.02					3.92			
Rejected		0					0			
Probability of fit		0.01					0.01			

$^{207}Pb^*/^{206}Pb^*$ model dates are calculated using the primordial Pb isotopic composition from Tatsumoto et al (1973).
MSWD = mean square of weighted deviates.
Probability of fit is the probability that, if the only reason for scatter is the analytical errors assigned to the data points, the scatter of the data points will exceed the amount observed for the data (Ludwig 2003).

Table 4. Summary of ages and cooling rates for H chondrites.

Meteorite	Petrologic type	Chondrule or whole rock Pb-Pb date (Ma)	2σ age error (Ma)	Phosphate Pb-Pb date (Ma)	2σ error (Ma)	Average cooling rate (K/Ma)[a]	2σ error (K/Ma)	^{40}Ar-^{39}Ar age (Ma)[b]
Ste. Marguerite	H4	4566.7[c, d]	1.6	4562.7[c, f]	0.7	74	43	4532 ± 16
Richardton	H5	4562.7[e, f]	1.7	4550.7[e, f]	2.6	24.7	12	4495 ± 11
Estacado	H6	4546.0[f, g]	18	4492.0[f]	15	5.5	3.2	4435 ± 5
		4527.6[f, h]	6.3			8.3	5.0	

[a]Average cooling rates are calculated using IsoplotEx 3.00 program (Ludwig 2003), Pb-Pb ages (this study) and closure temperatures for chondrules and for phosphates (Amelin et al. 2005).
[b]Comparison with $^{40}Ar/^{39}Ar$ ages of whole rock for Ste. Marguerite and Richardton, and of whole rock, feldspar, and pyroxene for Estacado from Trieloff et al. (2003).
[c]$^{207}Pb/^{206}Pb$ dates are from Göpel et al. (1994).
[d]Pb-Pb model date.
[e]$^{207}Pb/^{206}Pb$ dates are from Amelin et al. (2005).
[f]Pb-Pb isochron date.
[g]Chondrule residue-second wash isochron.
[h]Chondule-matrix radiogenic Pb transfer isochron.

within error, with ages of chondrules in primitive chondrites (Amelin and Krot, Forthcoming), and suggests either that the peak of metamorphism in the H-chondrite parent body occurred early (before 4560 Ma), or that the highly metamorphosed part of the H-chondrite parent body did not experience extensive Pb loss during the peak of metamorphism (in the latter case the single-stage Pb-Pb date approaches T0), or both. This result is not surprising, considering the known old age of metamorphic minerals (Ca phosphates) in H chondrites with moderate degrees of metamorphism (Göpel et al. 1994).

Between T2 and T3, the temperature in the parent body was still sufficiently high to allow migration of Pb in pyroxene. Under these conditions, radiogenic Pb that forms in chondrules leaks into the matrix and is embraced by the matrix minerals that have affinity to Pb (e.g., sulfides or feldspar). In this case, Pb isotopic dating of pure chondrule material would yield the timing of cessation of Pb diffusion (T3). Fractions enriched in matrix components relative to the bulk chondrite, that have preferentially gained the early radiogenic Pb, would have elevated $^{207}Pb/^{206}Pb$ ratios, and would yield anomalously high $^{207}Pb/^{206}Pb$ model dates (the model of metamorphic transfer of radiogenic Pb between chondrules and chondritic matrix is presented in Appendix 3).

The model of radiogenic Pb transfer provides a plausible explanation for the data for magnetic fractions #13R and 14R if these fractions are enriched in matrix material relative to the bulk chondrite. Four data points of chondrules and magnetic fractions are co-linear. The regression through these fractions, if interpreted as a single-stage isochron, gives the date of 4532 ± 16 Ma, distinctly younger than the bulk meteorite isochrons. This line may be interpreted as a radiogenic Pb transfer isochron, which gives the age of the termination of Pb diffusion in chondrules. Acid-washed bulk chondrites (fractions #19R–22R) also plot on this line, in agreement with prediction of the radiogenic Pb transfer model. If the whole rock points are included, we get a more precise date of 4527.6 ± 6.3 Ma (MSWD = 1.11) from this eight-point isochron (Fig. 5).

We have now two estimates of the age of Estacado chondrules: 4546 ± 18 Ma from the internal residue-second leachate isochron dates for the two chondrule fractions, and 4527.6 ± 6.3 Ma from the radiogenic Pb transfer isochron (Figs. 4 and 5). These dates agree, although marginally, at the 95% confidence level. The difference between the underlying assumptions of these two age estimates is not in accepting or rejecting the fact of the radiogenic Pb transfer, but in the assumed origin of common Pb in the chondrule analyses. In the first estimate, we implicitly assume that the common Pb comes from incomplete removal of soluble "interstitial material," or from the chondrules themselves; in the second estimate, the common Pb is assumed to be from adhering bits of matrix, which have also gained some radiogenic Pb that diffused out of the chondrules before T3. The future identification, separation, and dating of additional well-preserved chondrules will resolve the uncertainty between these two dates.

Cooling Rates of H Chondrites

To estimate the cooling rate of a particular part of a metamorphic complex (for example, the source region of a meteorite) from the ages of chondrules and phosphates, we need to know the closure temperature for diffusion of Pb and U in these minerals. Amelin et al. (2005) estimated the closure temperatures for these chronometers in H5 chondrites as 1055 ± 106 K for chondrules and 759 ± 56 K for phosphates (errors are 2σ) on the basis of experimentally determined diffusion coefficients (Cherniak 2001; Cherniak et al. 1991), and the size and geometry of pyroxene and Ca phosphate crystals. Since the compositions and the range of crystal sizes of pyroxene and phosphate minerals—the parameters that influence the closure temperature—are broadly similar in H5 and H6 chondrites, we use the same values of the closure temperatures in this study. We used a simple linear approximation to determine the cooling rates because only two points (phosphates and silicates) are available for calculations. Therefore, our estimates of the cooling rates involve the simplistic assumption that the cooling rate of a specific meteorite was constant between two temperatures. In reality, cooling rates could vary with time. From these closure temperatures, together with the phosphate isochron age of 4492 ± 15 Ma, and the estimates of the chondrule age of 4546 ± 18 Ma from the internal residue-second wash isochron, or 4527.6 ± 6.3 Ma from the radiogenic Pb transfer isochron, we obtain cooling rates of 5.5 ± 3.2 Ma/°C, and 8.3 ± 5.0 Ma/°C, respectively.

The chondrule and phosphate ages, and the cooling rates calculated for Estacado can be compared to the ages and cooling rates of other H chondrites of different metamorphic grades determined by U-Pb dating using a similar approach. Phosphate and chondrule dates (or bulk silicate dates, if chondrule data are not available) for three selected H chondrites are presented in Table 4. Estacado has the youngest phosphate Pb-Pb isochron date among the dated chondritic meteorites (Göpel et al. 1994; Amelin et al. 2005), but this age is similar, within the error, to the reported Pb-Pb model phosphate age for Guareña (H6) (4504.4 ± 0.5 Ma) (Göpel et al. 1994). From the data presented in Table 4, it is clear that phosphate ages are decreasing from H4 type (4562.7 ± 0.7 Ma) to H6 type (4492.0 ± 15 Ma). Göpel et al. (1994) reported a similar pattern in Pb-Pb model ages of phosphates from a larger number of H4, H5, and H6 chondrites. Our date for Estacado phosphates corroborates the phosphate age pattern established by Göpel et al. (1994).

In addition, our data is also comparable with the results and conclusions by Trieloff et al. (2003). Their estimated ^{40}Ar-^{39}Ar date (4435 ± 5 Ma) for Estacado is correlated with

our phosphate Pb-Pb date in similar fashion as Ar-Ar and Pb-Pb dates for St. Marguerite and Richardton (Table 4 here; Table 1 in Trieloff et al. 2003).

The chondrule and bulk chondrite dates for Estacado, Richardton, and St.Marguerite are similar within the error of each other. For St. Marguerite (H4), only the model date of 4566.7 ± 1.6 Ma is available for the bulk chondrite, and this date is similar to the Pb-Pb isochron dates of chondrules from carbonaceous chondrites that were less affected by thermal metamorphism (Amelin et al. 2002; Amelin and Krot, Forthcoming). Chondrules in Richardton at 4562.7 ± 1.7 Ma are slightly younger than the oldest chondrules in carbonaceous chondrites (4566.6 ± 1.0 Ma in Allende [Amelin and Krot, Forthcoming]). The Estacado internal residue-second wash Pb-Pb date of 4546 ± 18 Ma is similar within the error with Richardton chondrules (Table 4).

The cooling rates of H chondrites (Table 4) decrease markedly with increasing metamorphic grade. The estimated average cooling rate of Estacado over the temperature range of 1055–759 K is about 2.5–4 times slower than that of Richardton, and about an order of magnitude slower than that of Ste. Marguerite.

Toward an Integrated Thermal Model of the H-Chondrite Parent Asteroid

Thermochronology data for the H5 chondrite Richardton has been used by Amelin et al. (2005) to constrain the timing of accretion, heating, and cooling of the parent asteroid of H chondrites following the approach developed by Ghosh et al. (2003). With our study the database for H chondrites of different metamorphic grades has expanded. Our findings for Estacado, which is the most metamorphosed type of H chondrites, provide additional information to constrain the thermal history of the H-chondrite parent body more precisely.

The variations of the ages and cooling rates observed among H chondrites are consistent with the theoretical predictions of the conventional “onion-shell” thermal model (Herndon and Herndon 1977; Minster and Allegre 1979; Miyamoto et al. 1982; and references therein). In this thermal model, the rate of heat loss, i.e., the cooling rate, in a particular layer of a chondritic parent body would decrease with depth. Our findings confirm that Estacado represents the innermost layer of a parent body (Trieloff et al. 2003), i.e., that it cooled at a slower rate than other layers in the same parent body (between 5.5 ± 3.2 Myr/°C and 8.3 ± 5 Myr/°C) (Table 4).

There are several important conditions that need to be addressed before confirming this model of the thermal history of the asteroid.

1. We need to understand whether the variations in the extent of metamorphic recrystallization, which are used to assign chondrites to certain petrologic types, are indeed related to the differences in the peak metamorphic temperature. This relationship, which is a cornerstone of the classical approach to chondritic metamorphism (Dodd 1981; McSween and Sears 1988), has been challenged by the experiments done by Wlotzka (2005) on the olivine/Cr-spinel and olivine-chromite thermometers, which suggest that equilibrated chondrites of types H4, H5, and H6 had the same average temperature (1039 K, 1047 K, and 1048 K, respectively). We need to understand the reasons of the discrepancy between mineral chronometers, and to verify their accuracy with respect to the absolute temperature scale, in order to assure accurate comparison to the temperature scale of diffusion.
2. Once the accuracy of mineral thermometry is verified, it would be necessary to perform precise measurements of metamorphic temperatures on the same chondrites that are being dated. This would eliminate a major uncertainty that comes from using estimated average metamorphic temperatures for each petrologic type. Indeed, the use of petrologic types as identifiers of metamorphic conditions in thermochronology studies should be avoided, because the petrologic types of chondrites represent a rather crude division of a continuum of physical conditions of metamorphism into a small number of types.
3. Several uncertainties are related to the determination of the rates of diffusion. The most important uncertainty comes from the application of diffusion coefficients measured in nearly perfect crystals to polycrystalline mineral aggregates with complex textures, such as chondrules. The diffusion along the grain boundaries can be as important as volume diffusion, or even more important, but we are not aware of experimental studies of diffusion in polycrystalline solids, which would provide a direct indication to the relative roles of these mechanisms of migration.
4. There is also a room for improvement in the isotopic dating of components of chondrites. Most important is developing an even more efficient way of removing common Pb and eliminating related sources of uncertainties (Amelin 2006). An interesting possibility is dating the peak of metamorphism of H6 chondrites using whole rock analyses. This approach to dating is promising, but its success depends on developing the right strategy of sampling.

CONCLUSIONS

Some results of this Pb-Pb study of H6 meteorites could have been foreseen, whereas the others came out as a surprise. The ages of phosphates from the H6 chondrite Estacado are younger than the previously published ages of phosphates in H5 and H4 chondrites, and the estimated cooling rate of

Estacado is slower than the cooling rates of H chondrites with a lower degree of metamorphism. These features are consistent with the "onion-shell" model of the H-chondrite parent asteroid, previously suggested on the basis of phosphate U-Pb geochronology for a series of H chondrites with various degrees of metamorphism.

A more surprising result is that two out of four studied H6 chondrites contain phosphates with unradiogenic Pb, whereas chondrules and/or whole rocks of all four of these meteorites contain radiogenic Pb after acid leaching. Another unexpected result is the observation that radiogenic Pb, lost from chondrules while Pb diffusion in pyroxene was still fast, has probably settled in certain domains in the chondrite matrix. Magnetic separation of a crushed meteorite can produce fractions enriched in these matrix domains, which yield anomalously old single-stage Pb-Pb dates. Understanding of these phenomena would require a detailed study of Pb and U distribution and migration in highly metamorphosed H chondrites on a microscopic scale.

Several issues should be addressed before confirming the "onion-shell" model for the H-chondrite parent body. The discrepancies between peak metamorphic temperatures established by various mineral thermometers need to be resolved, diffusion and other mechanisms of element migration in polycrystalline solids must be better understood, and dating techniques should be further improved. The database of Pb-Pb isochron ages for phosphates and chondrules for H4, H5, and H6 also has to be expanded. Future studies in meteorite chronology and thermometry will help to determine how, and when, the parent asteroids of chondritic meteorites were assembled, heated, and cooled.

Acknowledgments–We would like to thank Drs. L. Nyquist, M. Trieloff, M. Bizzaro, and associate editor Dr. C. Floss for constructive reviews. We are grateful to the following people at the Geological Survey of Canada in Ottawa who helped us at various stages of this study: Dr. Richard Herd provided meteorites, Pat Hunt helped with imaging and X-ray mapping, Julie Peressini provided guidance in mineral separations, Tom Pestaj, Linda Cataldo, Diane Bellerive, and Carole Lafontaine helped the first author to master mount preparation, clean chemistry techniques, and mass spectrometry. We thank Dr. John Blenkinsop from Carleton University for insightful comments and inspiring discussions. This work was supported by an Undergraduate Student Research Award to A. Blinova from the National Science and Engineering Research Council (NSERC) of Canada.

Editorial Handling—Dr. Christine Floss

REFERENCES

Amelin Y. 2006. The prospect of high-precision Pb isotopic dating of meteorites. *Meteoritics & Planetary Science* 41:7–17.

Amelin Y. and Davis W. J. 2006. Isotopic analysis of lead in sub-nanogram quantities by TIMS using a ^{202}Pb-^{205}Pb spike. *Journal of Analytical Atomic Spectrometry* 21:1053–1061.

Amelin Y. and Krot A. N. 2007. Pb isotopic age of the Allende chondrules. *Meteoritics & Planetary Science* 42. This issue.

Amelin Y., Krot A. N., Hutcheon I. D., and Ulyanov A. A. 2002. Pb isotopic ages of chondrules and calcium-aluminum-rich inclusions. *Science* 297:1678–1683.

Amelin Y., Stern R., and Krot A. N. 2003. Distribution of U, Th, Pb, and Nd between minerals in chondrules and CAIs (abstract #1200). 34th Lunar and Planetary Science Conference. CD-ROM.

Amelin Y., Ghosh A., and Rotenberg E. 2005. Unravelling the evolution of the chondrite parent asteroids by precise U-Pb dating and thermal modeling. *Geochimica et Cosmochimica Acta* 69:505–518.

Blinova A. 2006. Constraining the cooling history of the H-chondrite parent body by precise U-Pb dating of phosphates and chondrules from an H6 chondrite. B.Sc. thesis, Department of Earth Sciences, Carleton University, Ottawa, Canada.

Blinova A., Amelin Y., and Samson C. 2006. U-Pb dating of phosphates and chondrules in H6 chondrites (expanded abstract, paper #17). 13th Annual Conference of the Canadian Aeronautics and Space Institute, Montreal.

Cherniak D. J. 2001. Pb diffusion in Cr diopside, augite, and enstatite, and consideration of the dependence of cation diffusion in pyroxene on oxygen fugacity. *Chemical Geology* 177:381–397.

Cherniak D. J., Landford W. A., and Ryerson F. J. 1991. Lead diffusion in apatite and zircon using ion implantation and Rutherford backscattering techniques. *Geochimica et Cosmochimica Acta* 55:1663–1673.

Dodd R. T. 1981. *Meteorites: A petrologic-chemical synthesis*. Cambridge: Cambridge University Press. 368 p.

Faure G. 1986. *Principles of isotope geology*, 2nd ed. New York: John Wiley & Sons. 608 p.

Gale N. H. and Mussett A. E. 1973. Episodic uranium-lead models and the interpretation of variations in the isotopic composition of lead in rocks. *Reviews of Geophysics and Space Physics* 11:37–86.

Ghosh A., Weidenschilling S. J., and McSween H. Y., Jr. 2003. Importance of the process in asteroidal thermal evolution: 6 Hebe as an example. *Meteoritics & Planetary Science* 38:711–724.

Göpel C., Manhes G., and Allegre C. 1994. U-Pb systematics of phosphates from equilibrated ordinary chondrites. *Earth and Planetary Science Letters* 121:153–171.

Grady M. M. 2000. *Catalogue of meteorites*, 5th ed. Cambridge: Cambridge University Press. 690 p.

Grimm R. E. 1985. Penecontemporaneous metamorphism, fragmentation, and reassembly of ordinary chondrite parent bodies. *Journal of Geophysical Research* 90:2022–2028.

Herndon J. M. and Herndon M. A. 1977. Aluminum-26 as a planetoid heat source in the early solar system. *Meteoritics* 12: 459–465.

Krot A., Amelin Y., Cassen P., and Meibom A. 2005. Young chondrules in CB chondrites from a giant impact in the early solar system. *Nature* 436:989–992.

Lodders K. 2003. Solar system abundances and condensation temperatures of the elements. *The Astrophysical Journal* 591: 1220–1247.

Ludwig K. R. 1993. PBDAT—A computer program for processing Pb-U-Th isotope data, version 1.24. United States Geological Survey Open-File Report 88-542, revision of June 22, 1993. pp. 1–33.

Ludwig K. R. 2003. Isoplot/Ex version 3.00, a geochronological

toolkit for Microsoft Excel. Berkeley Geochronology Center Special Publication #4.

Lugmair G. W. and Galer S. J. C. 1992. Age and isotopic relationships among the angrites Lewis Cliff 86010 and Angra dos Reis. *Geochimica et Cosmochimica Acta* 56:1673–1694.

McSween H.Y., Jr. and Sears D. W. G. 1988. Thermal metamorphism. In *Meteorites and the early solar system*, edited by Kerridge J. F. and Matthews M. S. Tucson, Arizona: The University of Arizona Press. pp. 102–113.

Minster J.-F. and Allegre C. J. 1979. ^{87}Rb-^{87}Sr chronology of H chondrites: Constraints and speculations on the early evolution of their parent body. *Earth and Planetary Science Letters* 42: 333–347.

Miyamoto M., Fujii N., and Takeda H. 1981. Ordinary chondrite parent body: An internal heating model. Proceedings, 12th Lunar and Planetary and Science Conference. pp. 1145–1152.

Reiners P. W., Ehlers T. A., and Zeitler P. K. 2005. Past, present, and future of thermochronology. In *Low-temperature thermochronology: Techniques, interpretations, and applications*, edited by Reiners P. W. and Ehlers T. A. Reviews in Mineralogy and Geochemistry vol. 58. Chantilly, Virginia: Mineralogical Society of America. pp. 1–18.

Scott E. R. D., and Rajan R. S. 1981. Metallic minerals, thermal histories and parent bodies of some xenolithic, ordinary chondrite meteorites. *Geochimica et Cosmochimica Acta* 45: 53–67.

Slater-Reynolds V. and McSween H. Y., Jr. 2005. Peak metamorphic temperatures in type 6 ordinary chondrites: An evaluation of pyroxene and plagioclase geothermometry. *Meteoritics & Planetary Science* 40:745–754.

Stacey J. S. and Kramers J. D. 1975. Approximation of terrestrial lead isotope evolution by a two-stage model. *Earth and Planetary Science Letters* 26:207–221.

Stöffler D., Keil K., and Scott E. R. D. 1991. Shock metamorphism of ordinary chondrites. *Geochimica et Cosmochimica Acta* 55: 3845–3867.

Tatsumoto M., Knight R. J., and Allegre C. J. 1973. Time difference in the formation of meteorites as determined from the ratio of lead-207 to lead-206. *Science* 180:1279–83.

Tera F. 2003. A lead isotope method for the accurate dating of disturbed geologic systems: Numerical demonstrations, some applications and implications. *Geochimica et Cosmochimica Acta* 67:3687–3716.

Tera F. and Carlson R. W. 1999. Assessment of the Pb-Pb and U-Pb chronometry of the early solar system. *Geochimica et Cosmochimica Acta* 63:1877–1889.

Trieloff M., Jessberger E. K., Herrwerth I., Hopp J., Fiéni C., Ghélis M., Bourot-Denise M., and Pellas P. 2003. Structure and thermal history of the H-chondrite parent asteroid revealed by thermochronometry. *Nature* 422:502–506.

Wlotzka F. 2005. Cr spinel and chromite as petrogenetic indicators in ordinary chondrites: Equilibration temperatures of petrologic types 3.7 to 6. *Meteoritics & Planetary Science* 40:1673–1702.